

Structure and properties of self-assembled fluorocarbon–silica nanocomposites

Carlos Rodríguez-Abreu ^{a,b,*}, Pablo M. Botta ^c, José Rivas ^c, Kenji Aramaki ^d,
Manuel Arturo López Quintela ^b

^a *Institut d'Investigacions Químiques i Ambientals de Barcelona, Consejo Superior de Investigaciones Científicas (IIQAB/CSIC),
Jordi Girona, 18-26, 08034 Barcelona, Spain*

^b *Departamento de Química Física, Facultad de Química, Universidad de Santiago de Compostela, E-15782 Santiago de Compostela, Spain*

^c *Departamento de Física Aplicada, Facultad de Física, Universidad de Santiago de Compostela, E-15782 Santiago de Compostela, Spain*

^d *Graduate School of Environment and Information Sciences, Yokohama National University, Tokiwadai 79-7,
Hodogaya-ku, Yokohama 240-8501, Japan*

Received 13 November 2006; received in revised form 22 June 2007

Available online 11 September 2007

Abstract

The formation of fluorocarbon–silica nanocomposites by the self-assembly of a fluorinated surfactant and aminoalkoxysilane coupling agents was studied by X-ray diffraction, electron microscopy, NMR spectroscopy and thermal analysis. The prepared materials possess a lamellar nanostructure consisting of non-crystalline fluorinated and condensed silica layers, the latter being very thin. The prepared materials show interesting properties for applications, such as hydrophobicity, thermal stability, high content of aminopropyl groups and low dielectric constant (≈ 2.8), which is almost independent on frequency. Moreover, the dielectric response can be interpreted in the framework of the Maxwell–Wagner model.

© 2007 Elsevier B.V. All rights reserved.

PACS: 81.07.Pr; 81.16.Dn; 61.10.Nz; 81.70.Pg

Keywords: X-ray diffraction; Nanocomposites; NMR; MAS-NMR and NQR; Organic–inorganic hybrids; Sol–gels (xerogels); Calorimetry

1. Introduction

Nanostructured hybrid materials combining organic and inorganic functions have drawn attention from the research community in the last years because their interesting properties and potential applications. Self-assembly is a ‘bottom–up’, low energy method used to prepare such materials, usually assisted by amphiphilic compounds [1]. Among them, fluorinated surfactants show special features.

They are highly hydrophobic and reduce the surface tension of aqueous solutions to an extent which is unattainable with hydrocarbon surfactants [2–4]. Moreover, they form aggregates at lower concentrations [5] and have high chemical and thermal stability [6]. Fluorocarbon surfactants have been used as structure directors for the synthesis of mesoporous silica [7–10] and also for the formation of ordered composites through complexation with polyelectrolytes [11]. The functionalization of silica with fluorocarbon chains offers possibilities for applications such as protective coatings [12] and low dielectric constant materials for semiconductors [13]. Ultra-low dielectric constants (values lower than 2) have been achieved by high-porosity silica aerogels or xerogels [14,15]. However, the weak structural stability of these materials seems to be a serious lim-

* Corresponding author. Address: Institut d'Investigacions Químiques i Ambientals de Barcelona, Consejo Superior de Investigaciones Científicas (IIQAB/CSIC), Jordi Girona, 18-26, 08034 Barcelona, Spain. Tel.: +34 981563100x13009; fax: +34 981595012.

E-mail address: craqci@iiqab.csic.es (C. Rodríguez-Abreu).

itation for the employed manufacturing processes. In this way hybrid materials could be an interesting alternative for dielectric applications because the component with low dielectric constant is an organic compound instead of air, which should significantly improve the mechanical properties of the devices.

In previous publications [16,17] the formation of lamellar organic–inorganic hybrids by using hydrocarbon surfactants and aminosilane coupling agents was reported. Here, we present a similar path for the preparation of hybrid fluorocarbon–silica nanocomposites with very thin silica sheets and a hydrophobic surface, which can have potential applications such as protective coatings, insulators and ion adsorption [18]. Several techniques are used to study their structure and properties, such as X-ray diffraction, electron microscopy, nuclear magnetic resonance (NMR), thermal analysis, and dielectric measurements.

2. Experimental

2.1. Materials

Perfluorooctane sulfonic acid, designated as $C_8F_{17}SO_3H$, was obtained as a gift from Mitsubishi Materials (Japan). Tetraethyl orthosilicate (TEOS, 98%) was supplied by Sigma–Aldrich (USA). 3-Aminopropyltriethoxysilane (APTES, 99%) was purchased from Tokyo Kasei Kogyo Co. Ltd. (Japan). Deionized water was used in the experiments.

2.2. Sample preparation

$C_8F_{17}SO_3H$ and APTES (for sample FLS-1) were mixed in a 1:1.5 mol ratio and then water was added so that its final concentration was 70 wt%. The readily precipitated solid was recovered by filtration, washed and dried for 24 h at 70 °C. Sample S-1 (pure silica) was prepared by mixing TEOS and HCl 5 M in a mass ratio 5/93. The obtained gel was washed and dried for 24 h at 70 °C.

Millipore water was used in all the experiments.

2.3. Characterization

X-ray scattering spectra were taken with a Philips 1710 diffractometer using $Cu K\alpha$ radiation.

Thermogravimetric analysis (TGA) (Perkin Elmer TGA 7) was conducted in air at a heating rate of 5 °C/min to monitor the calcination process of composites.

Differential scanning calorimetry (DSC) was carried out with a Perkin Elmer DSC 7 at a heating rate of 5 °C/min.

^{29}Si MAS-NMR spectra of powdered samples were recorded at the magic angle in an Inova 750 spectrometer. The spinning frequency was 7 kHz. Time intervals of 5 s between successive accumulations were selected for the Si nuclei and 1600 accumulations were recorded. Tetramethylsilane was used as internal reference.

Dielectric properties of the prepared materials at room temperature were determined by means of the parallel-plate capacitor method. The capacitance (C) and loss factor (D) were measured with a commercial Agilent 16451B test fixture coupled to an Agilent 4284A LCR-meter, in a frequency range of 10^4 – 10^6 Hz. Prior to the measurement, the powder sample was compacted into circular pellets (typically 10 mm in diameter and 1 mm thick), applying a uniaxial pressure of 6 Ton/cm². The dielectric constant was calculated from the following expression:

$$\epsilon'_r = \frac{h}{A} \cdot \frac{C}{\epsilon_0},$$

where h is the thickness of the pellet (measured with a digital caliper), A is the contact area between the sample and the electrode, ϵ_0 is the permittivity of the free space (8.85×10^{-12} F/m) and C is the capacitance obtained at each frequency.

3. Results and discussion

3.1. X-ray diffraction

To compare the structure of the organic and composite material, X-ray diffraction spectra of $C_8F_{17}SO_3H$ and FLS-1 are shown in Fig. 1. Three reflections were obtained at relatively small scattering angle for FLS-1, indicating the existence of a supramolecular structure. The positions of peak maxima correspond to d spacings with approximate ratios $d_1:d_2:d_3 = 1:2:3$, which can be assigned to a lamellar structure. In fact, this is a preferred structure in many fluorinated surfactant systems [5,19,20].

$C_8F_{17}SO_3H$ gives two sharp SAXS peaks with $d_1:d_2 = 1:2$, the first one associated to $d_1 = 2.7$ nm. Assuming also a lamellar structure for $C_8F_{17}SO_3H$, the length of $C_8F_{17}SO_3H$ molecules within the layers would be $d_1/2 = 1.35$ nm. The C_8F_{17} -chain length (in Å) in its extended conformation can be calculated from the equation [21]

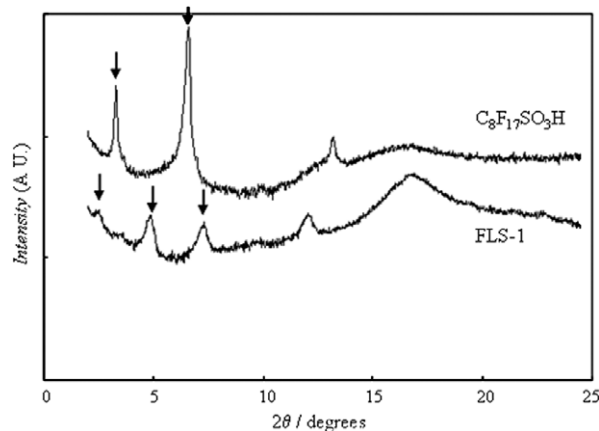


Fig. 1. X-ray diffraction patterns for pure $C_8F_{17}SO_3H$ and FLS-1 samples. For clarity of presentation, the intensity for $C_8F_{17}SO_3H$ was multiplied by an arbitrary factor. The arrows indicate reflections with a peak ratio corresponding to a lamellar structure.

$$l = 2.0 + 1.34n_F, \quad (1)$$

where n_F is the number of carbon atoms in the fluorinated chain. Then, $l = 1.30$ nm for $C_8F_{17}SO_3H$. Adding the contribution of $-SO_3H$ group (≈ 0.4 nm), we obtain 1.7 nm for the fully extended $C_8F_{17}SO_3H$ molecule. This value is larger than the obtained from X-ray diffraction ($d_1/2$); therefore, the chains might be either shrunk or interdigitated in the lamellar structure; the last type of arrangement is consistent with that proposed for bilayers in other fluorinated amphiphiles [22]. A tilted orientation of the molecules could be also possible.

On the other hand, for FLS-1 sample $d_1 = 3.6$ nm, a value much larger than that of pure $C_8F_{17}SO_3H$. The difference (0.9 nm) can be the contribution of aminosilane plus the condensed silica layer between the fluorocarbon chains. To our knowledge, this is the first time a nanocomposite with so thin silica layers is prepared.

In the wider angle region, $C_8F_{17}SO_3H$ gives only a small X-ray diffraction peak at $d = 0.67$ nm above an amorphous halo in the wide angle range, indicating the absence of crystalline order. This small peak probably corresponds to a higher order (fourth) reflection coming from the supramolecular lamellar structure. On the other hand, FLS-1 gives a small peak at $d = 0.73$ nm (which could be also assigned to a fifth order spacing of the lamellar structure) and a broad reflection at around $d = 0.53$ nm, which is typical of perflu-

orocarboxylic acids [12,23,24] in a disordered state. The apparent increase of the area of this broad peak when compared to the $C_8F_{17}SO_3H$ pattern can be attributed to some overlapping with the reflection of amorphous silica. The WAXS results indicate that the fluorinated chains remain in a disordered state in the hybrid FLS-1 sample.

A SEM image of FLS-1 (Fig. 2(a)) revealed a stacked arrangement of silica sheets morphologically related to the lamellar structure inferred from X-ray diffraction, which indicates a possible hierarchical structure. On the other hand, the embedded fluorocarbon makes the surface of the material (pellets) hydrophobic (Fig. 2(b)), which might be also interesting from the point of view of applications.

3.2. ^{29}Si NMR analysis

The ^{29}Si C-MAS spectrum of FLS-1 is presented in Fig. 3. Only one peak at -64 ppm (with a small shoulder at -66 ppm) is clearly resolved. No peak is found at -45 ppm, which is the chemical shift of neat, liquid APTES [25,26]. The peak at -64 ppm corresponds to R-Si silicons with three Si-O-Si linkages in aminoalkoxysilanes [25,27,28]. The absence of peaks at -49 ppm (one Si-O-Si linkage) and -58 ppm (two Si-O-Si linkages) indicates that the condensation of siloxane groups is practically complete. The condensation reaction might be favored by the preferred location of aminosilane groups in the confined layers forming the lamellar structure. No peak was found below -100 ppm, namely, there is no evidence of the presence of a pentacoordinate silicon, with a N-Si bond [27].

3.3. Thermal analysis

TGA data for FLS-1 is presented in Fig. 4a. There is a single and very well resolved thermal decomposition event starting at around 320 °C and finishing at around 520 °C. About 10 wt% of the original mass still remains at 700 °C. This roughly corresponds to the initial Si + O mass if the $C_8F_{17}SO_3H$ and APTES are assumed to be coupled following a 1:1 stoichiometry, which indicates that most silanes have condensed into a thermally stable siliceous structure, in agreement with NMR results. The decomposition temperature (≈ 410 °C from derivative data) is much higher than that of $C_8F_{17}SO_3H$ (≈ 130 °C) and similar to that of sodium perfluorooctane-1-sulfonate (information from suppliers). It suggests that aminosilane is strongly coupled to $C_8F_{17}SO_3^-$. The presence of aminosilane groups in the materials might be favorable for ion adsorption.

The DSC curve for FLS-1 (Fig. 4(b)) shows a broad endothermic peak with a minimum at 78 °C and associated with an enthalpy change of 30 J/g. The broadness of the peak is typical of non-crystalline solids, in agreement with X-ray diffraction results. Both the transition temperature and an enthalpy change of FLS-1 are much higher than those corresponding to $C_8F_{17}SO_3H$ sample (data not

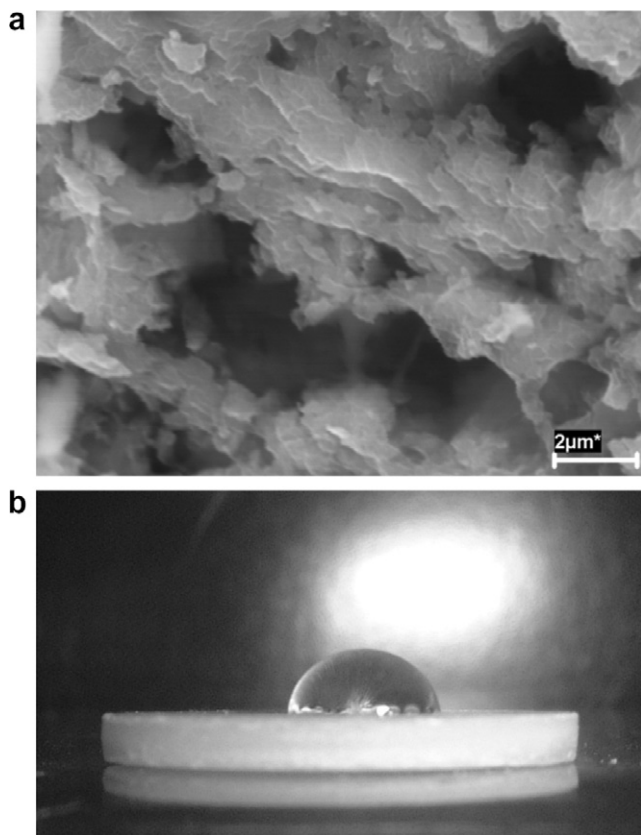


Fig. 2. (a) SEM image of FLS-1. (b) Photograph of a water droplet on a pellet of the hybrid fluorocarbon-silica material showing the hydrophobicity of the surface.

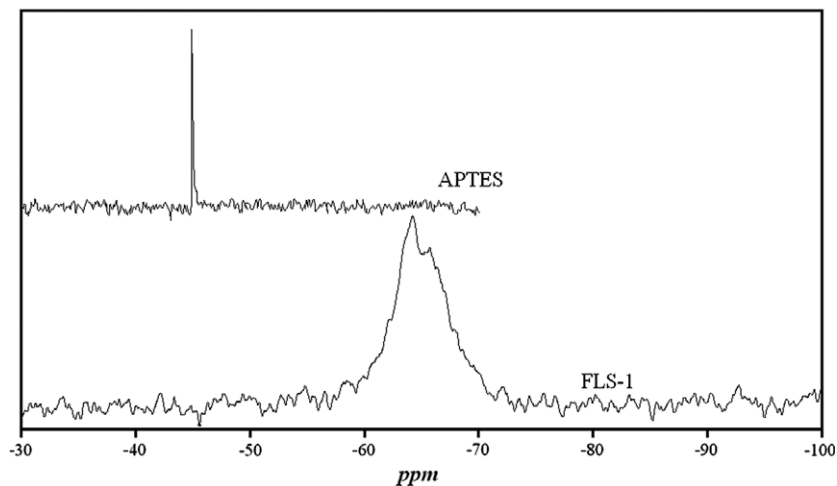


Fig. 3. ^{29}Si C-MAS spectrum of FLS-1 (bottom). The spectrum for neat APTES (top) is also included for comparison (adapted from Ref. [26]).

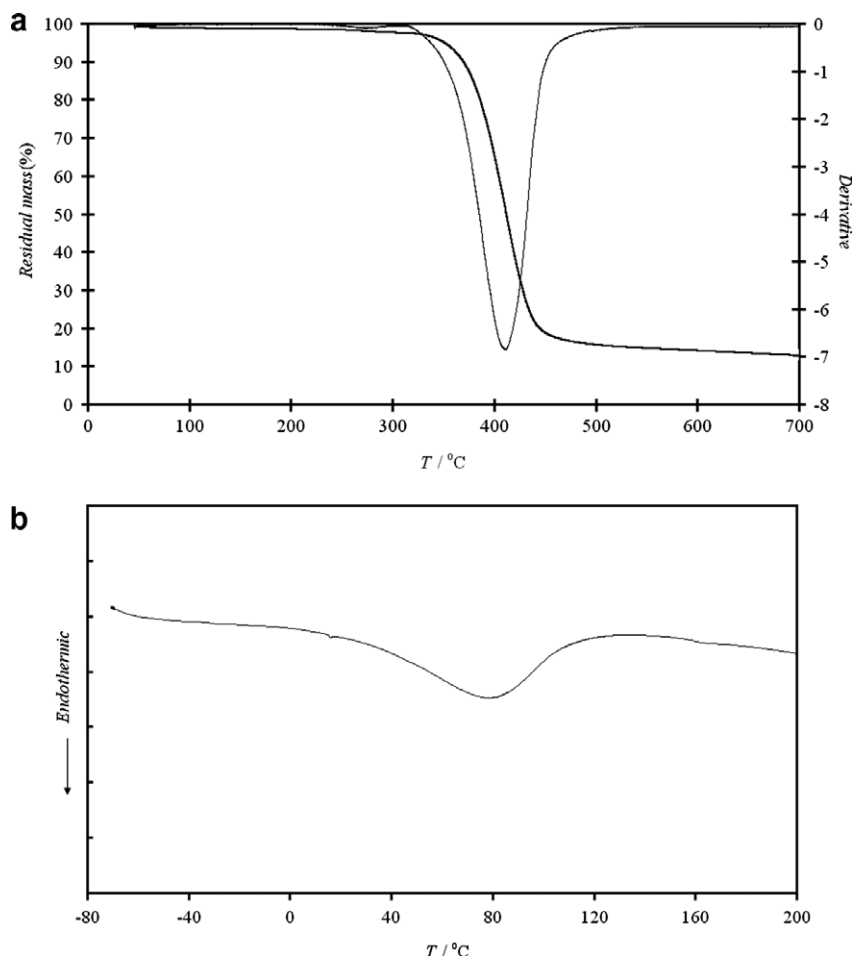


Fig. 4. (a) TGA and (b) DSC (heating curve) results for FLS-1.

shown), further confirming the strong organic–inorganic coupling in the hybrid material.

3.4. Structure of fluorocarbon–silica hybrids

Fig. 5 shows the hypothetical structure for the hybrid materials, which consists of alternating perfluorooctane

and condensed silica layers. It has been found [17] that during the early stages of the formation process of long chain organic acid-silica hybrids, the aminosilane acts as a counterion for the acid so that amphiphilicity drives the self-assembly. As hydrolysis and condensation of the aminosilane groups at the interface proceeds, the specific surface area and interfacial curvature decrease and there is a mor-

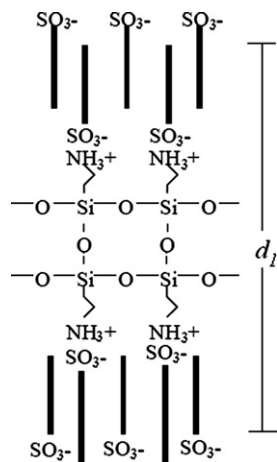


Fig. 5. Scheme of the possible lamellar structure in FLS-1 samples.

phological transition to sheet-like structures [17]. Taking into account the length of C–N, Si–C, C–C and Si–O bonds and typical bond angles, the thickness of the layers between fluorocarbon chains would be ≈ 1.1 nm, not much different than the value estimated from X-ray spectra.

3.5. Dielectric properties

Fig. 6 shows the real part of the relative dielectric permittivity, the dielectric constant ϵ'_r , as a function of frequency for samples FLS-1. Data for a sample without fluorocarbon (S-1) are also included for comparison. For FLS-1 an almost flat response can be observed, indicating the absence of any dielectric relaxation in the measured frequency range. This fact reveals that there are no silanol groups in the material structure, since the dipolar relaxation of SiOH should be noticed in the measured frequency range [29]. This behavior is in excellent agreement with the

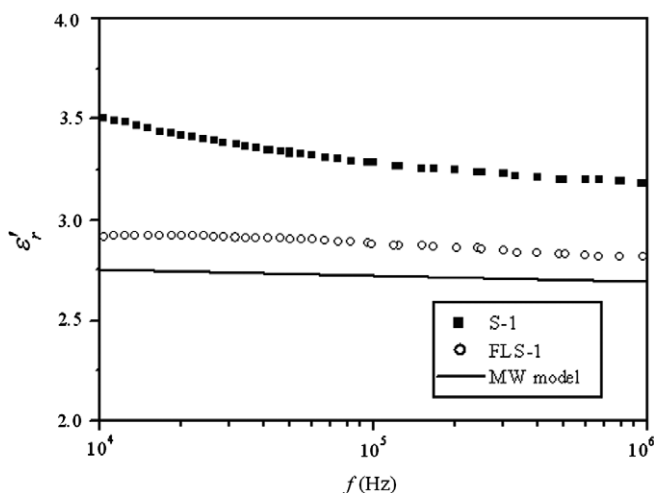


Fig. 6. Dielectric constant as a function of frequency for pure and fluorinated silica (samples S-1 and FLS-1, respectively). The line shows the response obtained by applying the MW model.

complete condensation of siloxane groups revealed by ²⁹Si NMR and TGA analysis. A comparison between curves corresponding to both S-1 and FLS-1 shows lower dielectric constant values for the fluorinated compound, which suggests the potentiality of this kind of hybrids to be employed as low-dielectric constant materials. In a very recent report [30], we showed that in hybrid materials synthesized from a nonionic fluorinated surfactant (instead of C₈F₁₇SO₃H) and a silica precursor (i.e. alkoxy silane), the dielectric constant is even lower (a minimum of about 2.15 was obtained), which we attribute to the absence of charged groups in the assemblies.

Measurements of loss factor, D , resulted in very low values (0.02–0.04) for all the frequencies, as expected for such insulating compounds.

Taking into account the lamellar structure schematized in Fig. 5, it is possible to apply the Maxwell–Wagner (MW) model [31] to predict the frequency response of the dielectric constant for such a hybrid system (for details on the equations, see Ref. [31]). This model is commonly applied to dielectrics composed by two or more phases with different ϵ'_r . The dielectric constants and volume fractions of each component are necessary to simulate the behavior of the composite. In this way, the studied material FLS-1 can be approached to a three-layer dielectric composed by perfluorooctane sulfonic acid, aminopropane and silicon oxide. The volume fractions of the corresponding phases were calculated from TGA and density data, giving 0.68, 0.24 and 0.08, respectively. For the sake of simplicity we used the equations for a two-component system, performing firstly the calculations for the layers composed by aminopropane and SiO₂, and afterwards, using the result obtained from this bilayer composite and that of perfluorooctane sulfonic acid. Changes in the order of these calculations did not produce significant differences in the obtained results. Dielectric constants of each component were taken from literature: $\epsilon'_r = 5.1$ for aminopropane [32] and $\epsilon'_r = 4.5$ for SiO₂ [33]. For perfluorooctane sulfonic acid the dielectric constant was approximated by the value commonly used for polytetrafluoroethylene ($\epsilon'_r = 2$). The response predicted by the model is shown in Fig. 6. A completely flat curve is observed as a consequence of the absence of a dielectric relaxation in the measured frequency range, in good agreement with the experimental results. Moreover the value obtained for the dielectric constant of the composite ($\epsilon'_r = 2.77$) is close to that measured for FLS-1 material ($\epsilon'_r = 2.92 - 2.82$), confirming the applicability of the MW model to this kind of lamellar systems. The slightly higher dielectric constant experimentally observed for the hybrid material could be related to the underestimation of ϵ'_r corresponding to perfluorooctane sulfonic acid, which was approximated to that of polytetrafluoroethylene. Due to the presence of a high-polarity group in C₈F₁₇SO₃H, the dielectric constant of this compound could be some higher than 2. If this is considered in the model, the agreement between the theoretical prediction and experimental measurement would be even better.

4. Conclusion

Hybrid fluorocarbon–silica materials with a lamellar nanostructure can be prepared by the cooperative self-assembly of perfluorooctane sulfonic acid strongly coupled with aminoalkoxysilanes. The silica layers in the materials are very thin, and contain a relatively high concentration of attached aminopropyl groups. Interestingly, the materials are thermally stable, hydrophobic and show a low dielectric constant (≈ 2.8), which is almost independent on frequency, as predicted by the Maxwell–Wagner model.

Acknowledgments

C.R. and P.M.B. gratefully acknowledge Ministry of Science and Education of Spain for the financial support (J. de la Cierva Program).

References

- [1] M. Lazzari, C. Rodríguez, J. Rivas, M.A. López-Quintela, *J. Nanosci. Nanotechnol.* 6 (2006) 892.
- [2] H. Kunieda, K. Shinoda, *J. Phys. Chem.* 80 (1976) 2468.
- [3] C. Rodríguez, H. Kunieda, Y. Noguchi, T. Nakaya, *J. Colloid Interf. Sci.* 242 (2001) 255.
- [4] C. Rodríguez, H. Kunieda, *J. Disper. Sci. Technol.* 26 (2005) 435.
- [5] J.C. Ravey, M.J. Stébé, *Colloid. Surf. A* 84 (1994) 11.
- [6] E. Kiss, *Fluorinated Surfactants and Repellants*, 2nd Ed., Marcel Dekker, New York, 2001.
- [7] J.L. Blin, P. Lesieur, M.J. Stebe, *Langmuir* 20 (2004) 491.
- [8] S.E. Rankin, B. Tan, H.J. Lehmler, K.P. Hindman, B.L. Knutson, *Micropor. Mesopor. Mater.* 73 (2004) 197.
- [9] J. Esquena, C. Rodríguez, C. Solans, H. Kunieda, *Micropor. Mesopor. Mater.* 92 (2006) 212.
- [10] S.C. Sharma, C. Rodríguez, J. Esquena, H. Kunieda, *J. Colloid Interf. Sci.* 299 (2006) 297.
- [11] A.F. Thünemann, *Prog. Polym. Sci.* 27 (2002) 1473.
- [12] A.F. Thünemann, *Langmuir* 16 (2000) 824.
- [13] G.J.A.A. Soler-Illia, P. Innocenzi, *Chem. Eur. J.* 12 (2006) 4478.
- [14] S.H. Hyun, J.J. Kim, H.H. Park, *J. Am. Ceram. Soc.* 83 (2000) 533.
- [15] L.W. Hrubesh, J.F. Poco, *J. Non-Cryst. Solids* 188 (1995) 46.
- [16] S. Che, A.E. Garcia-Bennett, T. Yokoi, K. Sakamoto, H. Kunieda, O. Terasaki, T. Tatsumi, *Nat. Mater.* 2 (2003) 801.
- [17] C. Rodríguez, T. Izawa, K. Aramaki, M.A. López-Quintela, K. Sakamoto, H. Kunieda, *J. Phys. Chem. B* 108 (2004) 20083.
- [18] T. Chujo, Y. Gonda, Y. Oumi, T. Sano, H. Yoshitake, *J. Mater. Chem.* 17 (2007) 1372.
- [19] J.C. Ravey, M.J. Stébé, S. Sauvage, C. Elmoujahid, *Colloid. Surf. A* 99 (1995) 221.
- [20] S. Mele, B.W. Ninham, M. Monduzzi, *J. Phys. Chem. B* 108 (2004) 17751.
- [21] F. Giulieri, M.P. Krafft, *Colloid. Surf.* 84 (1994) 121.
- [22] T. Imae, K. Funayama, M.P. Krafft, F. Giulieri, T. Tada, T. Matsumoto, *J. Colloid Interf. Sci.* 212 (1999) 330.
- [23] A.F. Thünemann, D. Ruppelt, H. Schnablegger, J. Blaul, *Macromolecules* 33 (2000) 2124.
- [24] B. Ren, Z. Tong, X. Liu, C. Wang, F. Zeng, *Langmuir* 20 (2004) 10737.
- [25] G.S. Caravajal, D.E. Leyden, G.R. Quinting, G.E. Maciel, *Anal. Chem.* 60 (1988) 1776.
- [26] H. Ni, D.J. Aaserud, W.J. Simonsick Jr., M.D. Soucek, *Polymer* 41 (2000) 57.
- [27] H.J. Kang, F.D. Blum, *J. Phys. Chem.* 95 (1991) 9391.
- [28] E.J.R. Sudholter, R. Huis, G.R. Hays, N.C.M. Alma, *J. Colloid Interf. Sci.* 103 (1985) 554.
- [29] A. da Silva, P. Donoso, M.A. Aegerter, *J. Non-Cryst. Solids* 145 (1992) 168.
- [30] C. Rodríguez, P.M. Botta, J. Rivas, K. Aramaki, M.A. López-Quintela, *Colloid. Surf. A* 298 (2007) 284.
- [31] A. Von Hippel, *Dielectrics and Waves*, Artech House, London, 1954.
- [32] W.T. Cronenwett, L.W. Hoogendoorn, *J. Chem. Eng. Data* 17 (1972) 298.
- [33] R.D. Shannon, *J. Appl. Phys.* 73 (1993) 348.